





High Isolation Low Profile MIMO Antenna for 5G Applications

Muhammad Nasir, Talha Baber, Muhammad Abdullah, Muhammad Husnain Aslam University of Engineering and Technology Lahore Faisalabad Campus

* Correspondence: Muhammad Nasir, Muhammad.nasir@uet.edu.pk

Citation | Nasir. M, Baber. T, Abdullah. M, Aslam. M. H, "High Isolation Low Profile MIMO Antenna for 5G Applications", IJIST, Vol. 07 Issue. 02 pp 907-915, May 2025

DOI | https://doi.org/10.33411/ijist/202572907915

Received | April 16, 2025 **Revised** | May 18, 2025 **Accepted** | May 20, 202 **Published** | May 22, 2025.

his article focuses on the multi-input multi-output (MIMO) antenna with smaller dimensions and improved isolation between the ports which results in good performance and is suitable for modern wireless communication systems, especially USB dongle and 5G mobile applications. Two main problems with the conventional antennas are (i) Large height between the top to ground plate and (ii) Smaller isolation between the ports. These two problems are carefully addressed in the proposed design. The height in the proposed antenna is minimized up to 4mm between the top and to ground plate. Further achieved isolation is more than -18dB by introducing a novel type of periodic slots in the ground plate of the antenna. The antenna structure consists of a ground plate and two top plates, each with defined dimensions. The parameters are optimized using software for the best performance of the antenna to ensure efficient signal transmission and reception. The proposed antenna aims to explore the impact of dimension parameters like impedance matching and fractional bandwidth and isolation between the ports. The antenna resonates for 4.5GHz to 5.75GHz frequency bandwidth. The return loss for impedance bandwidth is below -20dB. The antenna is simulated on software and fabricated on substrate FR4. The simulated and measured results are compared which indicates that this antenna with high isolation and good impedance bandwidth is a more suitable candidate for 5G mobile applications. Compared to the conventional same-class antenna, the proposed antenna has good performance with minimized dimensions.

Keywords: Isolation; radiation patterns; return loss; DGS (defected ground structure), PIFA (planer inverted F antenna), SAR (specific absorption rate)





























Introduction:

MIMO technology plays a crucial role in exploiting multiple signal paths for data transmission and reception. This technology is a valuable resource to achieve optimal performance such as bandwidth, isolation, gain, and compactness to meet rigorous requirements. It is essential to carefully design the antenna orientation and spacing to maximize gain and ensure proper isolation for space-constrained devices. PIFAs are preferred for their simplicity, compact size, low cost, planar structure, and reduced SAR, making them ideal for portable applications [1][2]. MIMO antenna has the capability of handling multipath fading with spatial diversity in the system [3][4]. Multiple methods are used to attain antenna diversity such as pattern diversity polarization and spatial diversity. A flexible polyimide substrate with a dielectric constant of 3.5 is utilized for isolation enhancement between 4 4element MIMO antenna arrays [5]. A compact dual port diversity gain planner inverted F antenna for LTE applications was designed with isolation up to 15 dB and ECC is 0.5 whereas the height between the top to ground plate is about 7.5mm [6]. A circular patch radiator was incorporated to enhance the impedance bandwidth, achieving a 2.6 GHz bandwidth that covers the frequency range from 37.7 to 40.3 GHz. Radiators for the array are developed without any decoupling structures, yet they effectively minimize coupling between the elements, as reported in [7].

Recently to compete with the growing demand and enhance the capacity of the 5th generation mobile communication a wider bandwidth is a key element. The latest applications like Smart cities, virtual reality, and autonomous vehicles are feasible in recent 5th generation technology due to high capacity of up to 20 Gbps with latency of almost 1ms [8][7][9][10][11]. Moreover, a dielectric resonator with an array of 4 elements is suggested in [12] for isolation improvement. In order to reduce mutual coupling between radiating elements, the elements are placed strategically on opposite sides of a common substrate [13]. Achieving optimal performance, particularly in terms of bandwidth and isolation in MIMO antennas remains a major challenge in current research. Moreover, for high frequency MIMO communication systems with broad bandwidth are special advantages like high data rates and signal reliability. This enhancement makes it better suited for applications that demand robust and highperformance operation within the millimeter-wave spectrum. The proposed antenna is a MIMO antenna with a smaller structure and high isolation. A new defected ground structure (DGS) technique is used to enhance isolation. The theoretical model of the antenna is analyzed on HFSS software. The results of the proposed antenna structure indicate that this antenna has a better performance compared to conventional same-class antennas. This manuscript consists of the methodology, results and discussion, comparative study and finally concluding remarks.

Novelty:

The distinctive aspects of the proposed antenna are summarized as follows:

- The height between the top and to ground plate is minimized to 4mm resulting in a low profile, compact design.
- The isolation is enhanced by implementing the innovative defective ground plate structure.
- This antenna with smaller apertures and good performance is the best candidate for portable wireless communication.

Objectives:

In conventional antennae maintaining the size while getting efficient performance is critical.

The reduction in the larger gap of antenna elements from the ground plate to the top plate and maintaining minimal isolation and ECC is a substantial challenge. These problems are



minimized in this study, which is caused by improving signal reliability and coverage significantly.

Methodology:

This section provides a detailed explanation of the design steps and methodologies used for the proposed low-profile MIMO antenna. It defines requirements, design specifications, antenna parameters, simulation and performance analysis, optimization strategies, analyzation of the model, iterative refinement, and validation of required results.

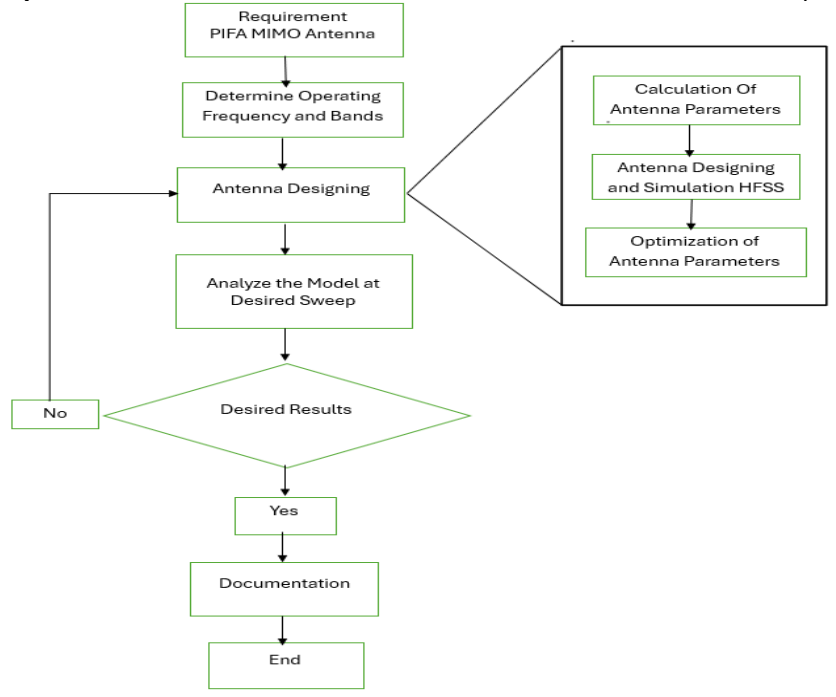


Figure 1. Flow diagram of methodology

The low-profile MIMO antenna architecture combines an ultra-compact form factor fit for contemporary 5G devices with a well-crafted multi-element structure meant to achieve maximum electromagnetic performance. The antenna system consists of some primary functional components, each carefully sized and positioned to achieve specific performance characteristics through controlled electromagnetic interactions.

The proposed antenna is comprised of a ground plate and two top plates as antenna elements arranged parallel to each other. The rectangular single-layer PCB (printed circuit board) serves as a ground plate with relative dielectric constant 4 (FR4) measuring length (Lg) 55 mm and width (Wg) 24mm generates the required image currents for appropriate antenna operation, maintains steady reference potential for the radiating components, and offers efficient shielding from backward radiation. The two top plates with high-conductivity copper sheets of 0.5mm thickness and measuring length (L1, L2) 16mm and width (W1, W2) 10mm, placed 4mm apart from each other and placed at a height of 4mm from the ground plate as illustrated in Figure 2.

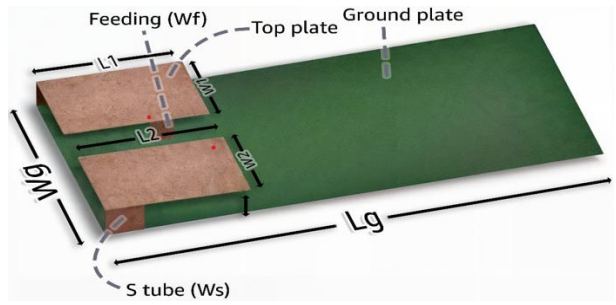


Figure 2. Layout and parametric description of the proposed antenna



A key impedance-matching feature that greatly improves the broadband performance of the proposed antenna design is the shunt stub implementation. The equation (1) discussed in [14] is used for initial calculations of the dimension parameters of the proposed antenna for center frequency. Furthermore, this model is simulated in HFSS software to optimize performance through parametric study.

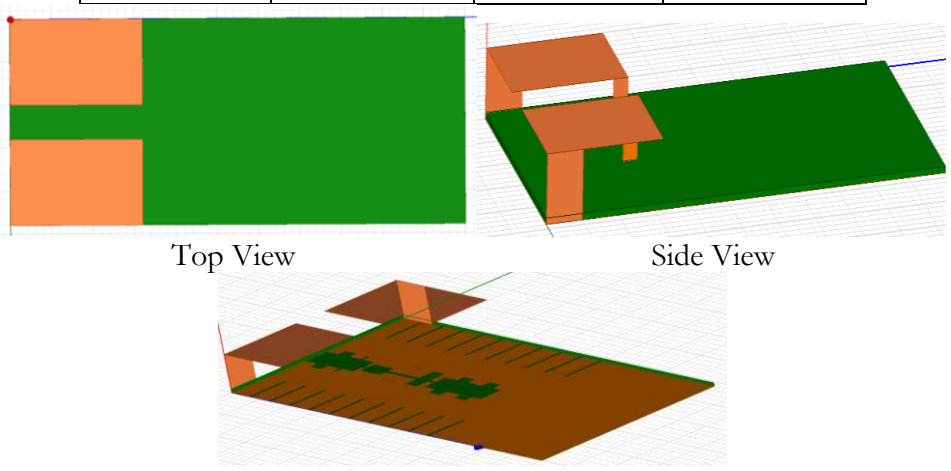
$$f_0 = \frac{c}{{}_{3W+5.6L+3.7h-3W_f-3.7Ws-4.3L_h-2.5Ls}}$$
(1)

Where W is the width, h is the height between the top to the ground plate, shunt plate width is W_s , the separation between feeding and shunt is L_b , feeding plate width is W_f , the position of shunt stub Ls.

The two top plates are placed facing each other at the feeding end of the ground plate. Each element has its own separate feeding port and shorting stub. The rectangular $5 * 5mm^2$ stub for top plate 1 lies at one side of the ground plate while the same size tube is placed on the other side of the ground plate for top plate 2. The top of this stub is connected to the top plate (first element) and the bottom side of this stub is connected to the copper of the ground plate. Both PIFA elements are fed by using $2 * 4mm^2$ rectangular microstrip from ground to top shown in Figure 3. The antenna's dimensional parameters are discussed in Table 1.

Table 1 Dimension parameters of the proposed antenna

Description	Length(mm)	Description	Length(mm)
Lg	55	L2	16
Wg	24	W2	10
L1	16	Ws	5
W1	10	h	4



Assembled Structure

Figure 3. 3D images of antenna top view, side view, and assembled structure.

The complete model is simulated using HFSS software. The model is analyzed for the frequency sweeping of 3.5 to 6 GHz bandwidth. The return loss and isolation of ports S11, S22, and S12 are observed respectively. A distinctive periodic 20 slots has been added at the side ends of the bottom ground plate. Each slot is 5mm in length and 1mm in width. The use of a well-tuned Defected Ground Structure (DGS) under the radiating components generates extra capacitive coupling that essentially reduces the Q-factor of the antenna, hence extending its frequency response. The current distribution due to these slots' changes density near short circuit stubs as shown in figure 4.

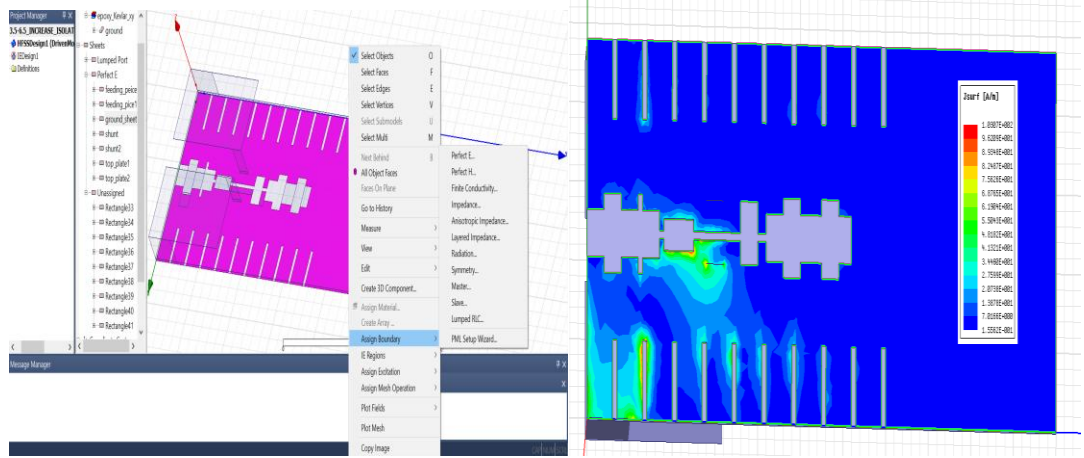


Figure 4. Simulated Pictures of the proposed antenna ground plate (bottom view) **Results and Discussion:**

The results obtained from low-profile MIMO antenna are discussed in this section. In Figure 5 return loss of both ports is shown with names S11 and S22. S11 is for port one and S22 is for port 2. The return loss of both ports is below -10dB in working bandwidth. At the central frequency, they are -20dB indicating good impedance matching. The similarity in the graphs of S11 and S22 verifies that both antenna elements exhibit similar characteristics. In Figure 5, the isolation (S12)graph provides information about the isolation between the ports.

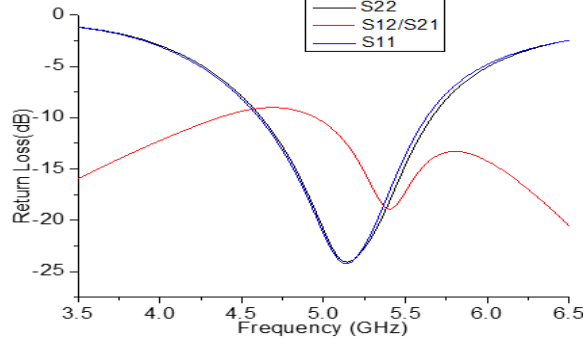


Figure 5. Return Loss Port one (S11), Return Loss Port two (S22), and S12 is Isolation between the ports.

Without compromising the structural integrity of the ground plane, the Defected Ground Structure (DGS) pattern consists of precisely dimensioned rectangular slots arranged in a periodic configuration caused by increased isolation of 10dB at the central frequency. The isolation for overall working bandwidth is below -10dB and near the central frequency is almost -20dB. In Figure 6, the impedance parameters are studied where real and imaginary parts of the antenna are discussed. At the center frequency, the real part is almost 50 Ω and the imaginary part is zero. The given results show that at working frequency antennas provide good impedance matching.

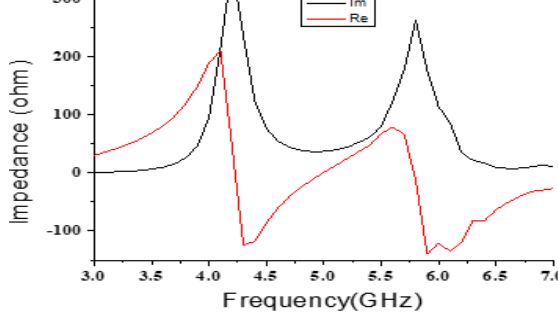


Figure 6. Real and imaginary parts of impedance VS frequency



The radiation pattern of this antenna is discussed in Figure 7 where the radiation patterns polar diagram for 0-360 degrees is presented, it can be seen that for both ports of proposed antenna elements with strength ranges confined to $\pm 0.5 \, dB$ and radiation yield maintained over 82% across the operating bandwidth, the frequency response of the antenna shows extraordinary stability. In this figure 7, 2D simulated radiation patterns for both elements have pattern diversity in the working frequency ranges of proposed antenna elements.

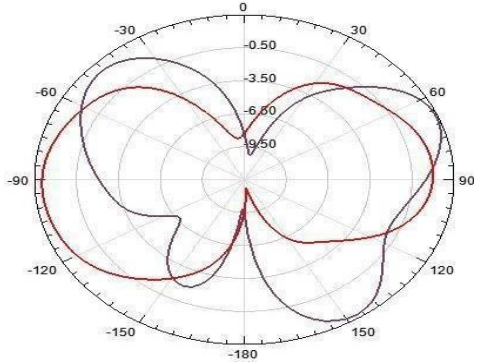


Figure 7. 2D radiation patterns polar diagram for both elements of the proposed antenna

As in the MIMO antenna system, isolation between the ports is a key performance indicator that indicates the measurement of separation and reduction in mutual coupling between the ports. There are some other parameters of the MIMO antenna that must be in acceptable ranges like ECC (envelop correlation coefficient) and diversity gain. Figure 8 explains these parameters, The envelope correlation coefficient of the MIMO antenna in Figure 8(a) is equal to zero which is near to ideal value for the entire frequency bandwidth. Figure 8 (b) indicates that the total active reflection coefficient is less than -10 dB. Figure 8 (c) explains the diversity gain of the elements of the antenna which is comparable to the theoretical value of almost 10dB.

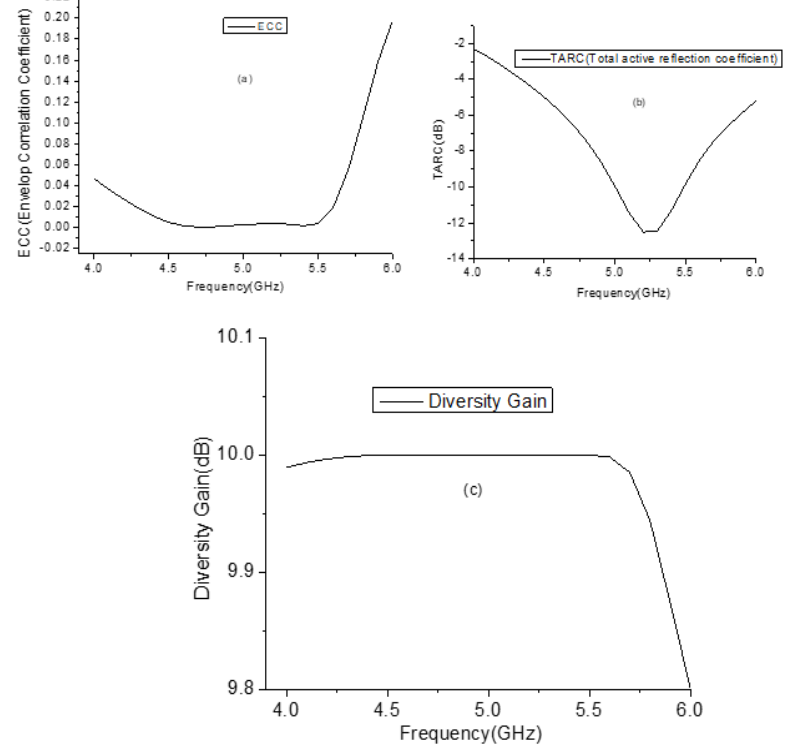


Figure 8 (a)ECC (Envelope Correlation Coefficient), (b) TARC (Total Active Reflection Coefficient), and (c)DG (Diversity Gain),



The resonant frequency and isolation results can be shifted with the different materials of the PCB. Figure 9 (a) discussed the improvement in isolation with the defective ground, and figures 9(b) and (c) discussed that isolation and central frequency shift at a lower frequency by increasing the relative dielectric constant respectively.

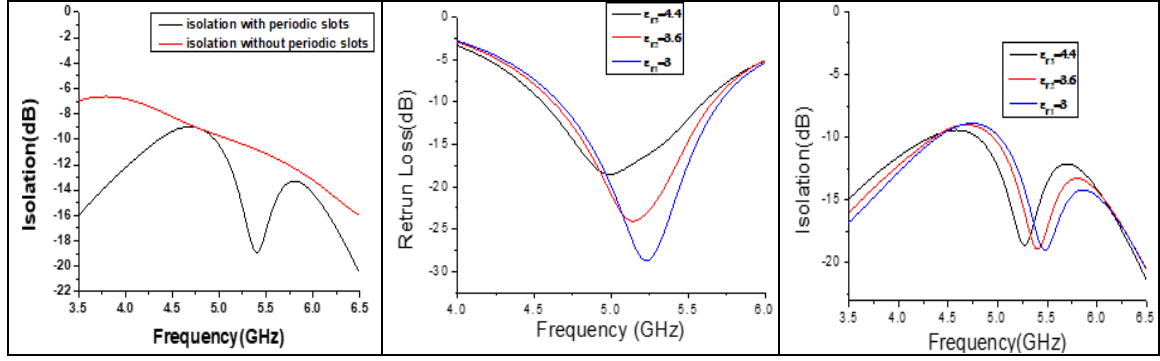


Figure 9 (a) Isolation with and without defected ground (b) isolation with different dielectric constants (c) central frequency with different dielectric constants

This improvement in isolation and broad bandwidth MIMO with smaller thickness makes the proposed antenna more novel in structure and the best antenna as compared with conventional antennas.

This is part of the novelty of the proposed antenna structure.

Discussion on Comparative Study:

The comparison with previous work demonstrates the distinctiveness of this work and proves the originality of this research work. Table 2 compares the proposed work with the existing study, first, the height between the top plate and ground plate is 4 mm in low profile MIMO antenna whereas in conventional antenna it is more than 7mm. The 7mm height was a problem in conventional antennae because it was difficult to fit with a slim mobile PCB. Second, the ECC in the presented antenna has a significant improvement of 0.001 for working bandwidth whereas in the existing study, it is almost 0.1 to 0.05. Moreover, this antenna has a less complex design with improved isolation compared to conventional antennas for the same class.

Table 2 Comparison of proposed work with existing study

Ref. No.	Size	Frequency	Isolation	ECC	Design
	$(L \times H mm^2)$	(GHz)	(dB)		Complexity
[This Work]	24 × 4	4.5-5.75	11	0.001	Low
[6]	95×7	2.5-2.7	15	0.5	Low
[15]	30×7.5	3.3-4.2	10.5	0.08	High
[16]	40×7.5	3.4-5	21	0.11	High
[17]	30×7 ,	3.3-7.5	10	0.05	Moderate

Conclusion:

The low-profile MIMO antenna presented has double channel capacity with high port isolation and can be used in 5G mobile applications WLAN, Wi-Fi WiMAX, and USB dongle applications. In this antenna, the height between the top plate and to ground plate is 4 mm which makes this antenna more compact and like printed antennas. This antenna can fit easily with the latest slim mobile with outstanding impedance matching and effective power transmission, low return loss, and smaller thickness. The fractional bandwidth is 25% with isolation at a central frequency below -18dB. This antenna is a low-cost structure with high efficiency because it is designed with a simple PCB with a ground plate of 0.5mm thickness with FR-4 dielectric and a copper sheet top plate with 0.5mm thickness. The results indicate that the proposed antenna has better performance compared to the same class MIMO antennas. Stable and elliptical, radiation patterns guarantee the best signal coverage.



Furthermore, minimizing the mutual connection between the MIMO configuration's antenna parts, therefore guaranteeing effective functioning and maximum data transmission. These findings validate that, with great performance in a low-profile form factor, the suggested antenna is a feasible choice for incorporation into small 5G devices.

References:

- [1] M. R. Jahangir et al, "Mutual Coupling Reduction in Compact MIMO Antenna Operating in K-Band," *PMC*, 2023.
- [2] S. E. Didi, I. Halkhams, M. Fattah, Y. Balboul, S. Mazer, and M. El Bekkali, "Design of a 2×2 dual band 28/38 GHz MIMO antenna in millimeter band for 5G," Telkomnika (Telecommunication Comput. Electron. Control., vol. 22, no. 2, pp. 273–281, Apr. 2024, doi: 10.12928/TELKOMNIKA.V22I2.25268.
- [3] R. G. Vaughan and J. B. Andersen, "Antenna diversity in mobile communications," *IEEE Trans. Veh. Technol.*, vol. 36, no. 4, pp. 149–172, 1987, doi: 10.1109/T-VT.1987.24115.
- [4] A. A. I. & S. M. G. Mai. F. Ahmed, Mohamed I. Ahmed, "Quad-port 28/38 GHz Antenna with Isolation Improvement for 5G Wireless Networks," *J. Infrared, Millimeter, Terahertz Waves*, vol. 45, pp. 672–693, 2024, [Online]. Available: https://link.springer.com/article/10.1007/s10762-024-00993-y
- [5] J. Kulkarni, A. G. Alharbi, A. Desai, C. Y. D. Sim, and A. Poddar, "Design and Analysis of Wideband Flexible Self-Isolating MIMO Antennas for Sub-6 GHz 5G and WLAN Smartphone Terminals," *Electron. 2021, Vol. 10, Page 3031*, vol. 10, no. 23, p. 3031, Dec. 2021, doi: 10.3390/ELECTRONICS10233031.
- [6] Q. Rao and D. Wang, "A compact dual-port diversity antenna for long-term evolution handheld devices," *IEEE Trans. Veh. Technol.*, vol. 59, no. 3, pp. 1319–1329, Mar. 2010, doi: 10.1109/TVT.2009.2037884.
- [7] N. A. Abbasi et al., "High-Isolation Array Antenna Design for 5G mm-Wave MIMO Applications," J. Infrared, Millimeter, Terahertz Waves, vol. 46, no. 1, pp. 1–22, Jan. 2025, doi: 10.1007/S10762-024-01027-3/TABLES/3.
- [8] M. K. Khan, S. Liu, and M. I. Khan, "A Wideband Eight-Port MIMO Antenna with Reduced Mutual Coupling for Future 5G mm-Wave Applications," *Sensors 2025, Vol. 25, Page 484*, vol. 25, no. 2, p. 484, Jan. 2025, doi: 10.3390/S25020484.
- [9] A. S. S. & A. U. Z. Davood Zarifi, "A high-gain gap waveguide-based 16×16 slot antenna array with low sidelobe level for mm Wave applications," *Sci. Rep.*, vol. 14, no. 31458, 2024, [Online]. Available: https://www.nature.com/articles/s41598-024-83283-w
- [10] E. A. Soliman, A. Vasylchenko, V. Volski, G. A. E. Vandenbosch, and W. De Raedt, "Series-fed microstrip antenna arrays operating at 26 GHz," 2010 IEEE Int. Symp. Antennas Propag. CNC-USNC/URSI Radio Sci. Meet. Lead. Wave, AP-S/URSI 2010, 2010, doi: 10.1109/APS.2010.5561286.
- [11] M. Hussain *et al.*, "Design and Characterization of Compact Broadband Antenna and Its MIMO Configuration for 28 GHz 5G Applications," *Electron. 2022, Vol. 11, Page 523*, vol. 11, no. 4, p. 523, Feb. 2022, doi: 10.3390/ELECTRONICS11040523.
- [12] N. S. Murthy, "Improved isolation metamaterial inspired MM-wave mimo dielectric resonator antenna for 5G application," *Prog. Electromagn. Res. C*, vol. 100, pp. 247–261, 2020, doi: 10.2528/PIERC19112603.
- [13] I. U. Din, S. Ullah, N. Mufti, R. Ullah, B. Kamal, and R. Ullah, "Metamaterial-based highly isolated MIMO antenna system for 5G smartphone application," *Int. J. Commun. Syst.*, vol. 36, no. 3, p. e5392, Feb. 2023, doi: 10.1002/DAC.5392.
- [14] H. T. Chattha, Y. Huang, X. Zhu, and Y. Lu, "An empirical equation for predicting the resonant frequency of planar inverted-F antennas," *IEEE Antennas Wirel. Propag.*



- Lett., vol. 8, pp. 856–860, 2009, doi: 10.1109/LAWP.2009.2027822.
- [15] L. Sun, Y. Li, Z. Zhang, and H. Wang, "Self-Decoupled MIMO Antenna Pair with Shared Radiator for 5G Smartphones," *IEEE Trans. Antennas Propag.*, vol. 68, no. 5, pp. 3423–3432, May 2020, doi: 10.1109/TAP.2019.2963664.
- [16] L. Sun, Y. Li, Z. Zhang, and Z. Feng, "Wideband 5G MIMO Antenna with Integrated Orthogonal-Mode Dual-Antenna Pairs for Metal-Rimmed Smartphones," IEEE Trans. Antennas Propag., vol. 68, no. 4, pp. 2494–2503, Apr. 2020, doi: 10.1109/TAP.2019.2948707.
- [17] X. T. Yuan, Z. Chen, T. Gu, and T. Yuan, "A Wideband PIFA-Pair-Based MIMO Antenna for 5G Smartphones," *IEEE Antennas Wirel. Propag. Lett.*, vol. 20, no. 3, pp. 371–375, Mar. 2021, doi: 10.1109/LAWP.2021.3050337.



Copyright © by authors and 50Sea. This work is licensed under Creative Commons Attribution 4.0 International License.